Journal of The Electrochemical Society

A Critical Evaluation of the Advanced Electrolyte Model

A Critical Evaluation of the Advanced Electrolyte Model

E. R. Logan,[1] Erin M. Tonita,[1] K. L. Gering,[2] and J. R. Dahn [1,3,*,z]

[1] *Department of Physics and Atmospheric Science, Dalhousie University, Halifax, Nova Scotia B3H 3J5, Canada*
[2] *Department of Biological & Chemical Processing, Idaho National Laboratory, I daho Falls, Idaho 83415-3732, USA*
[3] *Department of Chemistry, Dalhousie University, Halifax, Nova Scotia B3H 4R2, Canada*

A fast and accurate method to obtain transport properties of electrolyte solutions for Li-ion batteries is of great interest for both screening potential electrolyte candidates and for use in physics-based models of Li-ion cells. The Advanced Electrolyte Model (AEM) considers various molecular-scale interactions in a chemical physics framework to calculate these electrolyte transport properties in a computationally inexpensive manner. Should these calculations match experiment well, the AEM would be an ideal tool for the rapid determination of transport properties for various electrolyte systems. This paper aims to evaluate the accuracy of the AEM against experimental viscosity and conductivity data for electrolytes of interest in lithium batteries. Recent measurements, as well as previous measurements of now-obsolete electrolyte systems, are compared to corresponding calculations from the AEM. The availability of accurate laboratory data has allowed for improved accuracy of the AEM theory, molecular parameters and related predictions of properties, in particular for certain systems with low concentrations of ethylene carbonate (i.e. low permittivity electrolytes), as well as systems containing the salt Li triflate or the solvent sulfolane. The model now provides accurate calculations for the transport properties of most of the different systems considered here.
 [DOI: 10.1149/2.0471814jes]

Manuscript submitted September 10, 2018; revised manuscript received October 10, 2018. Published October 25, 2018.

The transport properties of electrolyte solutions help determine whether an electrolyte is appropriate for a given electrochemical storage application. Further, measuring transport properties such as ionic conductivity and viscosity of an electrolyte as functions of temperature and the concentration of conducting salt can help determine the limiting operating conditions of a storage device (e.g. minimum operating temperature, maximum charging rate). In addition to the direct application of using electrolyte transport properties to screen for appropriate electrolyte systems, accurate concentration-dependent transport properties are required to accurately model the charge-discharge behavior of Li-ion cells.[1–4]

Given the widespread popularity of Li-ion batteries with non-aqueous organic electrolytes, transport properties for this class of electrolyte have been widely reported in the literature.[4–19] Many methods exist for measuring the basic transport properties of electrolytes such as viscosity and ionic conductivity. Experimental setups can be relatively simple and inexpensive. For example, Beaulieu et al. developed a system for measuring the dynamic viscosity of fluids using a simple Ostwald viscometer, but automated the collection of data as a function of temperature using computer vision (CV) software.[20] Even considering the relatively low complexity of measuring these quantities, the determination of electrolyte transport properties can be expensive due to the relatively large quantities of materials required for testing, and time-consuming. Further, measuring other transport properties such as transference number, diffusivity, and activity coefficient have proven to be difficult, and these quantities are still vastly underreported in the literature.[1–4] Therefore, a model that can accurately predict the full set of transport properties for a given electrolyte system would be extremely valuable to the Li-ion battery community and beyond.

The Advanced Electrolyte Model (AEM), developed by Kevin Gering at Idaho National Laboratory, uses a statistical-mechanics model based on the non-primitive non-restricted associative form of the Mean Spherical Approximation (NPNRAMSA).[21,22] By modeling molecular scale interactions (solvent-solvent, solvent-ion, ion-ion), the AEM can calculate a wide range of properties of an electrolyte, including, but not limited to: viscosity, conductivity, diffusivity, transport numbers, and activity coefficients. The model also calculates quantities related to ion association such as single ion, ion pair, and triple ion populations, and solvated ionic radii. Thermodynamic and kinetic quantities are also calculated, such as those tied to ion solvation, and solution permittivity is rigorously treated over composition and temperature. The AEM has previously been validated for a number of high-dielectric non-aqueous systems containing popular Li-ion battery solvents and salts such as propylene carbonate (PC), ethylene carbonate (EC), ethyl methyl carbonate (EMC), dimethyl carbonate (DMC), diethyl carbonate (DEC), $LiPF_6$, Li bis(oxalato)borate (LiBOB), Li bis(fluorosulfonyl)imide (LiFSI), and Li bis(trifluoromethylsulfonyl)amine (LiTFSI).[21,22] Recently, the validity of the AEM has been studied for two new classes of carbonate-based Li electrolytes: electrolytes containing aliphatic esters such as methyl acetate (MA), ethyl acetate (EA), methyl butyrate (MB), and methyl propionate (MP); and low permittivity electrolytes containing little to no EC.[6,7] These types of electrolytes are of interest for their abilities to improve rate capability and high voltage cycling, respectively, in Li-ion cells.[23–33]

It is important to demonstrate the validity of the AEM over a wide range of electrolyte systems. Further, to validate the AEM for many different solvents and salts beyond the primary species used in the Li-ion battery space will demonstrate the robustness of the AEM. Dudley et al. measured ionic conductivity for a vast number of Li electrolytes with many different combinations of solvents and Li salts, many of which are supported by the AEM.[5] If the AEM can correctly predict the conductivity (and other transport properties) of these electrolytes, it will add to its overall strength.

The purpose of this paper is to demonstrate the validity of the AEM for a larger set of electrolyte systems than has been previously considered, as well as to highlight areas where AEM calculations do not agree well with experimental results. Some effort has already been made to validate the AEM for a several systems, both aqueous and non-aqueous.[6,7,21,22] However, combining the work of Logan et al.[6,7] with Dudley et al.,[5] as well as with previously unreported data gives the opportunity to conduct a broad evaluation of the AEM's strengths and weaknesses for a large set of systems, both novel and obsolete. Further, calculations made using previous versions of the AEM software are compared to demonstrate the contributions made from experiment to improve the AEM to its present form, as well as the modeling difficulties associated with some of the more challenging systems.

Experimental

The electrolytes considered in this paper fall under three main classes. The first class consists of a common blend of carbonate solvents with 20% by weight of different co-solvents added. The base

*Electrochemical Society Fellow.
[z]E-mail: jeff.dahn@dal.ca

Table I. Electrolytes from Logan et al.[6,7] where experimental conductivity and viscosity is available. Systems where only ionic conductivity is available are marked by an asterisk*.

Salt	concentration (m)	solvent 1	solvent 2	solvent 3	1 mass %	2 mass %	3 mass %
$LiPF_6$	0–2.0	EC	EMC	-	0	100	-
$LiPF_6$	0–2.0	EC	EMC	-	10	90	-
$LiPF_6$	0–2.0	EC	EMC	-	20	80	-
$LiPF_6$	0–2.0	EC	EMC	-	30	70	-
$LiPF_6$	0–2.0	EC	EMC	MA	30	60	10
$LiPF_6$	0–2.0	EC	EMC	MA	30	50	20
$LiPF_6$	0–2.0	EC	EMC	MA	30	40	30
$LiPF_6$	0–2.0	EC	DMC	-	0	100	-
$LiPF_6$	0–2.0	EC	DMC	-	10	90	-
$LiPF_6$	0–2.0	EC	DMC	-	20	80	-
$LiPF_6$	0–2.0	EC	DMC	-	30	70	-
$LiPF_6$	0–2.0	EC	DMC	MA	30	60	10
$LiPF_6$	0–2.0	EC	DMC	MA	30	50	20
$LiPF_6$	0–2.0	EC	DMC	MA	30	40	30
$LiPF_6$*	1.2	EC:EMC:DMC 25:5:70 (v/v)	MA	-	80	20	-
$LiPF_6$*	1.2	EC:EMC:DMC 25:5:70 (v/v)	EA	-	80	20	-
$LiPF_6$*	1.2	EC:EMC:DMC 25:5:70 (v/v)	MF	-	80	20	-
$LiPF_6$*	1.2	EC:EMC:DMC 25:5:70 (v/v)	EF	-	80	20	-
$LiPF_6$*	1.2	EC:EMC:DMC 25:5:70 (v/v)	MP	-	80	20	-
$LiPF_6$*	1.2	EC:EMC:DMC 25:5:70 (v/v)	MB	-	80	20	-
$LiPF_6$*	1.2	EC:EMC:DMC 25:5:70 (v/v)	PN	-	80	20	-

solvent blend used here was EC:EMC:DMC 25:5:70 (v/v), and the various co-solvents used were: methyl acetate (MA), ethyl acetate (EA), methyl formate (MF), ethyl formate (EF), methyl propionate (MP), methyl butyrate (MB), and propionitrile (PN). $LiPF_6$ was used for all solvent blends. This information is summarized in Table I.

The second class of electrolytes considered here are various blends of EC, EMC, DMC, and MA with $LiPF_6$ as the conducting salt for various salt concentrations, reported in Logan et al.[6,7] The electrolyte formulations used here are given in Table I. Details about the suppliers and purities of the chemicals used here can be found in References 6 and 7.

The third class of electrolytes comes from the work of Dudley et al.[5] That work considered a wide range of non-aqueous Li electrolytes for use in Li batteries. The main solvents considered in this study were EC, PC, sulfolane, n-glyme solvents (glyme (dimethoxyethane, DME), diglyme, triglyme, tetraglyme), and γ-butyrolactone (GBL). The conducting salts considered by Dudley et al. were $LiAsF_6$, $LiPF_6$, $LiBF_4$, LiTFSI, and Li trifluoromethanesulfonate (Li triflate, LiTf). More solvents and salts were considered in Dudley et al., but not all are currently supported by the AEM. It should also be noted that while many of the solvents and salts studied in Dudley et al. are no longer being considered for state-of-the-art Li electrolytes, this data is still valuable to validate the AEM's calculations. The electrolyte solutions from Dudley et al. considered here are summarized in Table II. The sources and preparation methods of the chemicals used in Dudley et al. can be found in Reference 5.

Conductivity measurements.—For electrolytes falling under classes 1 and 2 (different co-solvents, and data from Logan et al., respectively),[6,7] conductivity was measured using a commercial conductivity meter (Hach model 3455). Each probe had an integrated PT1000 RTD to monitor the temperature of the electrolyte. Probes were calibrated in air and to a known standard (12.88 mS/cm, Hanna Instruments HI70030C). 14.5 mL of electrolyte was added to a custom-made stainless-steel holder under a fume hood. The probe was then sealed to the holder by an O-ring to limit electrolyte-air contact. The seal was maintained by using custom-made stainless-steel clamps. Sealed holders were then placed in a temperature controlled bath (VWR Scientific model 1151) filled with ethylene glycol. The temperature of the bath was varied between 0°C and 40°C, in increments of 10°C. The temperature of the bath was verified in this range using an external thermocouple thermometer (Omega HH802U), and found to be accurate to ±0.5°C between 0.0°C and 100.0°C. At each step, the electrolyte was allowed to equilibrate with the temperature of the bath for at least 40 minutes. Measurement accuracy was within ±2% of the measured conductivity value.

For the data in Dudley et al. (class 3), a two electrode conductivity cell with Pt electrodes was used. The conductivity measurements quoted in that work were accurate to ±5% of the measured value. The range of temperatures considered by Dudley et al. was −60°C to +80°C, however not all electrolytes were liquid over this full temperature range. Full details of the conductivity apparatus can be found in Ref. 5.

Viscosity measurements.—Viscosity measurements were recorded for the electrolytes in classes 1 and 2 (Table I). Viscosity was measured using an Ostwald viscometer (Sibata Scientific Technology, Japan). Two different sized viscometers were used in these experiments, with capillary diameters of 0.5 mm and 0.75 mm, respectively. The temperature of the electrolyte in the viscometer was controlled by a circulating bath (Thermo Scientific) filled with a water/ethylene glycol mixture. The viscometer was placed inside a triple walled glass Dewar where the mixture was circulated. An RTD attached to the surface of the viscometer measured the temperature of the electrolyte. Measurement of the viscosity was completed using computer vision (CV) software developed by Beaulieu et al.[20] Viscosity measurements were taken for temperatures ranging from 10°C to 40°C. Reproducibility of these measurements is typically within 1%. The raw data were interpolated to temperatures in 5 degree increments using a linear interpolation method in MATLAB. This routine introduces some additional error. Total uncertainty after the interpolation has been applied was taken to be 2%.

Advanced electrolyte model.—The AEM's approaches to viscosity and conductivity calculations have been published,[21,22] and emanate from various chemical physics terms derived for multi-member electrolytes. Central to these terms is the influence of ion solvation (free cations and anions) as well as solvated ion pairs and triple ions. For example, ion solvation introduces structure into electrolyte solutions that causes viscosity to increase, and it also increases the effective transport diameters of the ions past their bare values and has a direct impact on the magnitude of transference numbers. Ion solvation is also a key contributor to activity coefficients. Numerous factors are assigned to overall descriptions of viscosity and conductivity through

Table II. Electrolytes from Dudley et al.[5] containing various (mostly obsolete) solvents and Li salts. Only conductivity data is available for these systems. Note that solvents are measured in volume % rather than mass % as was done in Table I.

salt	concentration (M)	solvent 1	solvent 2	solvent 3	1 vol%	2 vol%	3 vol%
$LiAsF_6$	1.0, 4.0	DME	EC	PC	50	25	25
Li-Tf	1.0	DME	EC	-	50	50	-
Li-Tf	1.0	DME	PC	-	50	50	-
LiTSFI	1.0	DME	EC	-	50	50	-
LiTFSI	1.0	DME	PC	-	50	50	-
$LiAsF_6$	0.5, 1.0, 1.5, 2.0	EC	PC	-	15	85	-
$LiAsF_6$	0.5, 1.0, 1.5, 2.0, 3.0	EC	PC	-	50	50	-
$LiAsF_6$	1.0	EC	PC	-	70	30	-
$LiPF_6$	1.0	EC	PC	-	15	85	-
$LiPF_6$	1.0	EC	PC	-	50	50	-
Li-Tf	1.0	EC	PC	-	50	50	-
LiTSFI	1.0	EC	PC	-	50	50	-
LiBF4	1.0	EC	PC	-	50	50	-
$LiAsF_6$	1.0	EC	PC	diglyme	25	25	50
$LiAsF_6$	1.0	EC	PC	triglyme	25	25	50
$LiAsF_6$	1.0	EC	-	-	100	-	-
$LiAsF_6$	1.0	EC	DME	-	50	50	-
$LiAsF_6$	1.0	EC	triglyme	-	50	50	-
$LiAsF_6$	1.0	GBL	-	-	100	-	-
$LiAsF_6$	1.0	GBL	DME	-	50	50	-
LiTFSI	1.0	GBL	DME	-	50	50	-
$LiAsF_6$	0.2, 1.0	PC	-	-	100	-	-
$LiAsF_6$	1.0, 4.0	PC	DME	-	50	50	-
$LiAsF_6$	0.2, 0.5, 1.0, 1.5, 2.0	sulfolane	-	-	100	-	-
$LiAsF_6$	0.5, 0.75, 1.0	sulfolane	tetraglyme	-	50	50	-
$LiAsF_6$	1.0	sulfolane	tetraglyme	-	25	75	-
$LiAsF_6$	0.5, 0.75, 1.0, 1.5, 2.0	sulfolane	triglyme	-	50	50	-
$LiAsF_6$	1.0	sulfolane	triglyme	-	25	75	-
$LiAsF_6$	1.0	sulfolane	triglyme	-	75	25	-
LiTFSI	0.75	sulfolane	triglyme	-	50	50	-
LiBF4	0.5	sulfolane	triglyme	-	50	50	-
$LiAsF_6$	1.0	sulfolane	diglyme	-	50	50	-
$LiAsF_6$	1.0	sulfolane	diglyme	-	60	40	-
$LiAsF_6$	1.0	sulfolane	DME	-	50	50	-
$LiAsF_6$	1.0	sulfolane	DME	-	60	40	-
$LiAsF_6$	1.0	sulfolane	diglyme	DME	50	25	25
$LiAsF_6$	1.0	sulfolane	diglyme	triglyme	50	25	25
$LiAsF_6$	1.0	sulfolane	DME	triglyme	50	15	35
$LiAsF_6$	1.0	sulfolane	DME	triglyme	50	25	25
$LiAsF_6$	1.0	sulfolane	EC	-	50	50	-
$LiAsF_6$	1.0	sulfolane	EC	triglyme	25	25	50
$LiAsF_6$	1.0	sulfolane	EC	triglyme	40	20	40
$LiAsF_6$	1.0	sulfolane	EC	triglyme	45	10	45
$LiAsF_6$	1.0	sulfolane	EC	triglyme	50	25	25
$LiAsF_6$	1.0	sulfolane	PC	-	50	50	-
$LiAsF_6$	1.0	sulfolane	PC	triglyme	45	10	45
$LiAsF_6$	1.0	triglyme	-	-	100	-	-

the AEM. For example, key terms that influence conductivity include: solvent-ion interactions (ion solvation and "dielectric drag") and solvated ion sizes, ion-ion interactions (ion association and electrostatic interactions), solution permittivity, viscosity, counter-ion transport, ionic hopping and ionic random motion effects. Each of these terms has been rigorously developed and the previous citations should be consulted for a thorough technical discussion.

Results and Discussion

Low-viscosity co-solvents.—Figure 1 shows ionic conductivity as a function of temperature for electrolytes with 1.2 mol/kg (molal, m) $LiPF_6$ added to a solvent mixture of EC:EMC:DMC 25:5:70 (v/v) plus 20% by weight of different co-solvents. Different co-solvents are specified by plotting symbol and color. AEM calculations (version 2.17.5) are shown in Figure 1 as solid lines. Many of these co-solvents have shown promise to improve low temperature and high rate cycling compared to traditional electrolyte blends.[29–34] Of the different co-solvents studied, electrolytes with propionitrile (PN) have the highest conductivity. Several of these co-solvents give an increase in conductivity compared to the control electrolyte, including: MA, MF, EF, and EA. As shown previously, MP and MB do not provide any appreciable increase in conductivity when used as a co-solvent alongside carbonate solvents.[6,27,35]

Figure 2 shows (a) the absolute deviation, and (b) the percent deviation of AEM calculations from experimental conductivity measurements at 0°C, 20°C, and 40°C for the electrolytes presented in Figure 1. Absolute deviation is shown in addition to percent deviation to highlight cases where an artificially large percent deviation may occur when the nominal conductivity is small. In such cases, absolute deviation may become a better metric for evaluating the performance of the AEM compared to experiment. The dashed line in Figure 2b shows a deviation of 10% from experiment. In general, the AEM agrees well with experiment for these electrolytes; within uncertainty, the AEM calculations for electrolytes with the different co-solvents all have less than 10% deviation. The electrolytes containing the es-

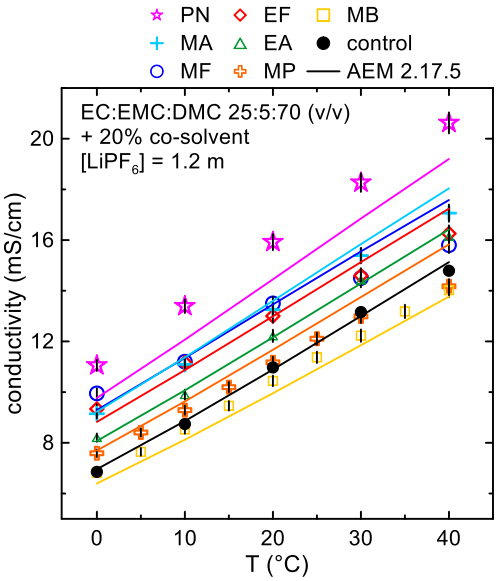

Figure 1. Ionic conductivity as a function of temperature for Li electrolytes composed of 1.2 m $LiPF_6$ in EC:EMC:DMC 25:5:70 (vol. %), containing 20% by weight of various different co-solvents, specified by plotting symbol. Calculations from AEM version 2.17.5 are given as solid lines.

ters MA, MB, and EA have good agreements with the AEM over the whole temperature range. There is some larger deviation from experiment with the PN-containing electrolyte, but this deviation is much smaller at higher temperature. Overall, it does not appear that there is an obvious temperature dependence in the AEM's agreement with experiment. Some electrolytes that agree well at one temperature have significantly higher deviations at another temperature (see, for example, the MP-containing electrolyte).

From the different co-solvents examined in Figures 1 and 2, PN gave the biggest increase in conductivity compared to the control electrolyte, followed by MA. More work has been done on Li-ion cells containing esters in the electrolyte than nitriles in the literature, so MA was pursued for further study in the work reported in Ref. 6. Further, a recent publication shows that Li-ion cells containing PN in the electrolyte perform poorly compared to other co-solvents.[36] Figure 3 shows viscosity measured as a function of $LiPF_6$ concentration for solvent compositions (a) EC:EMC 30:70, (b) EC:DMC 30:70, (c) EC:EMC:MA 30:60:10, (d) EC:DMC:MA 30:60:10, (e) EC:EMC:MA 30:50:20, (f) EC:DMC:MA 30:50:20, (g) EC:EMC:MA 30:40:30, and (h) EC:DMC:MA 30:40:30, all given in weight percent. Temperatures between 10°C and 40°C are shown. Calculations from two different versions of the AEM are given here: AEM version 2.17.2 is shown in dashed lines, and calculations from AEM version 2.17.5 are shown as solid lines. For electrolyte systems containing either EMC or DMC, adding MA to the system causes a decrease in viscosity over all temperatures and salt concentrations, as has been shown previously.[6] In general, both versions of the AEM capture the dependence of viscosity on both of these parameters quite well. However, it appears that the older version (2.17.2) slightly overestimates the viscosity of EMC-containing electrolytes, and slightly

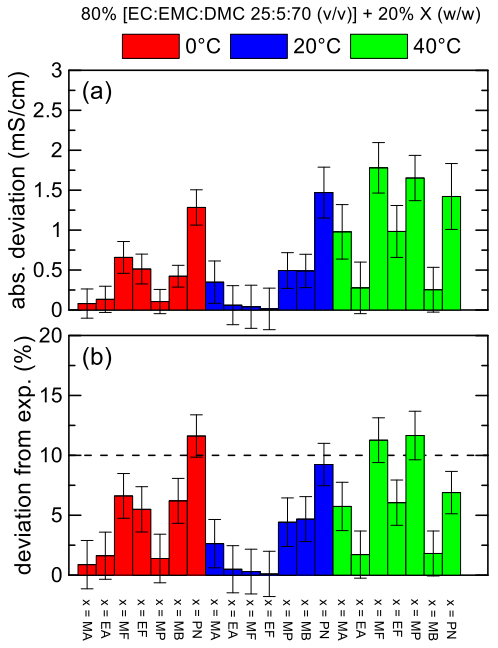

Figure 2. (a) Absolute deviation and (b) percentage deviation of the AEM (version 2.17.5) from experimental values of conductivity for the electrolytes presented in Figure 1, for different temperatures. A deviation of 10% is shown as a dashed line in panel (b).

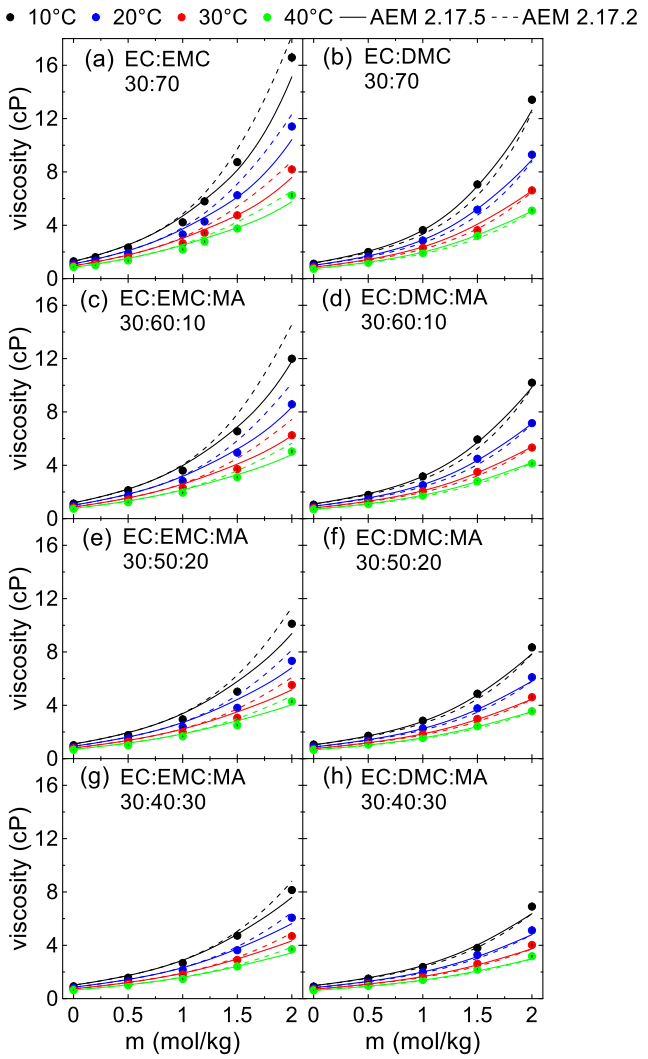

Figure 3. Viscosity as a function of $LiPF_6$ concentration for electrolytes with the solvent blends (a) EC:EMC 30:70, (b) EC:DMC 30:70, (c) EC:EMC:MA 30:60:10, (d) EC:DMC:MA 30:60:10, (e) EC:EMC:MA 30:50:20, (f) EC:DMC:MA 30:50:20, (g) EC:EMC:MA 30:40:30, and (h) EC:DMC:MA 30:40:30, all given in weight percent. Calculations from two different versions of the AEM are shown in solid and dashed lines, for AEM 2.17.5, and AEM 2.17.2, respectively.

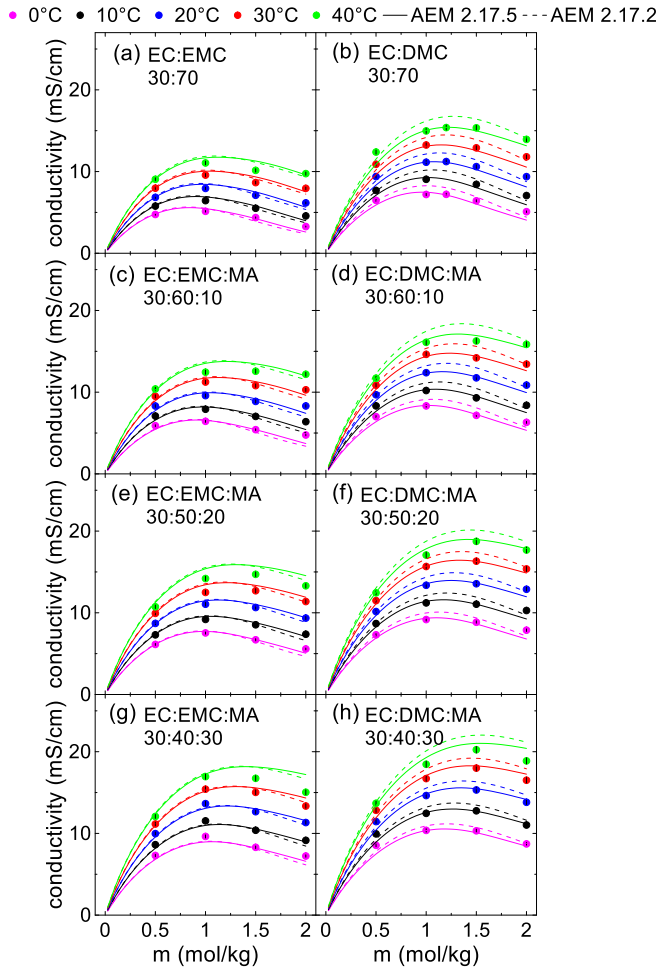

Figure 4. Ionic conductivity as a function of $LiPF_6$ concentration for electrolytes with the solvent blends (a) EC:EMC 30:70, (b) EC:DMC 30:70, (c) EC:EMC:MA 30:60:10, (d) EC:DMC:MA 30:60:10, (e) EC:EMC:MA 30:50:20, (f) EC:DMC:MA 30:50:20, (g) EC:EMC:MA 30:40:30, and (h) EC:DMC:MA 30:40:30, all given in weight percent. Calculations from two different versions of the AEM are shown in solid and dashed lines, for AEM 2.17.5, and AEM 2.17.2, respectively.

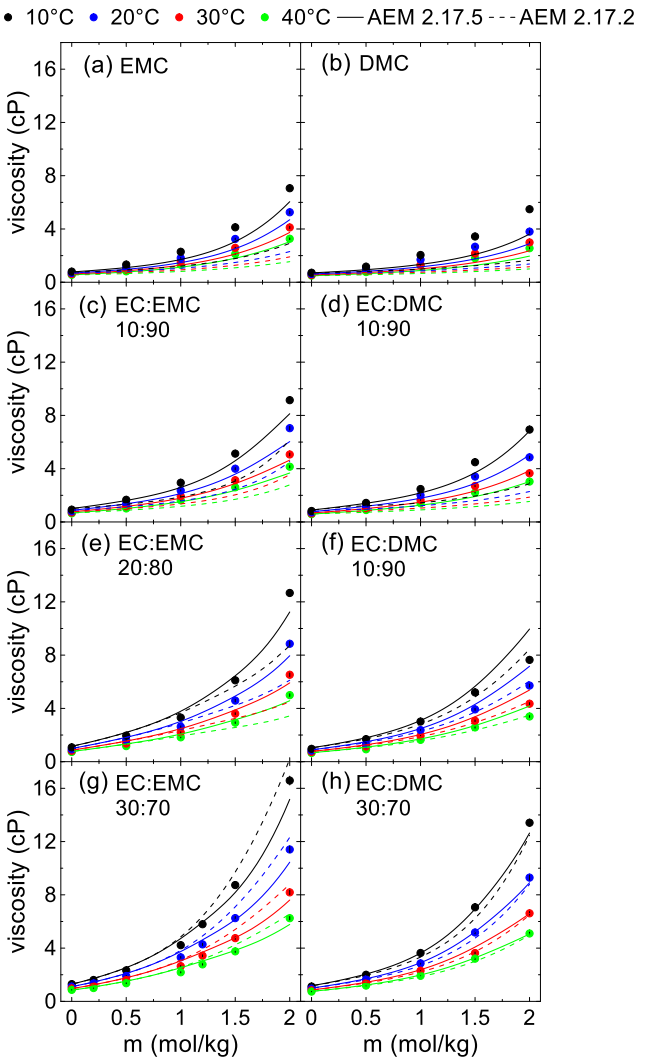

Figure 5. Viscosity as a function of $LiPF_6$ concentration for electrolytes with solvent blends (a) EMC, (b) DMC, (c) EC:EMC 10:90, (d) EC:DMC 10:90, (e) EC:EMC 20:80, (f) EC:DMC 20:80, (g) EC:EMC 30:70, and (h) EC:DMC 30:70, all in weight percent. Temperatures from 0°C to 40°C are shown. Calculations for AEM versions 2.17.2 and 2.17.5 are shown with dashed and solid lines, respectively.

under-estimates the viscosity of DMC-containing electrolytes. This discrepancy has been fixed in subsequent versions of the AEM. This was done by assigning more accurate molecular parameters to each of the solvent-ion combinations through standard reference ligand lengths and solvent residence times around ions. A more thorough discussion is given below.

Figure 4 shows ionic conductivity as a function of $LiPF_6$ molality for the solvent compositions (a) EC:EMC 30:70, (b) EC:DMC 30:70, (c) EC:EMC:MA 30:60:10, (d) EC:DMC:MA 30:60:10, (e) EC:EMC:MA 30:50:20, (f) EC:DMC:MA 30:50:20, (g) EC:EMC:MA 30:40:30, and (h) EC:DMC:MA 30:40:30, again given in weight percent. Calculations from two different AEM versions are shown: AEM 2.17.2 is shown as dashed lines, and AEM 2.17.5 is shown as solid lines. Like the viscosity data for this same set of electrolytes, AEM calculations for the conductivity of these systems agrees well with experiment. Very little difference is seen between AEM versions 2.17.2 and 2.17.5 for solvent blends containing EMC, while small improvements are made between versions for electrolyte solutions containing DMC.

Figures 5 and 6 show viscosity and ionic conductivity, respectively, for electrolyte solutions containing variable amounts of EC. In both Figures 5 and 6, panels (a) through (h) show solvent blends EMC, DMC, EC:EMC 10:90, EC:DMC 10:90, EC:EMC 20:80, EC:DMC 20:80, EC:EMC 30:70, and EC:DMC 30:70, again given in weight percent. In these Figures it can be seen that the previous version of the AEM (2.17.2) had poor agreement for electrolytes with low-permittivity solvent blends. For the viscosity data shown in Figure 5, AEM version 2.17.2 severely under-predicts the viscosity of electrolytes containing 0 or 10% EC by weight. This has been improved in subsequent versions, however when DMC is used as the sole solvent (Figure 5b) the AEM still under-predicts the $LiPF_6$-dependent viscosity to a degree. Similar trends are seen in the ionic conductivity for these electrolytes, as seen in Figures 6. In AEM version 2.17.2, the calculated conductivity for EC-free electrolytes does not capture the non-linear behavior that has been observed for these low-permittivity systems.[37–40] Further, for electrolytes with 10% EC (Figures 6c and 6d), AEM version 2.17.2 outputs unrealistic values for ionic conductivity. These significant discrepancies have been addressed in subsequent versions, and now the AEM is able to successfully predict the non-linear behavior seen at low Li-ion concentration in EC-free electrolytes. This improvement in the AEM for low-permittivity systems is due to revised theory for solution permittivity that includes the influence of ion pair dipoles on the total solution permittivity. The presence of these dipoles increases permittivity which causes a subse-

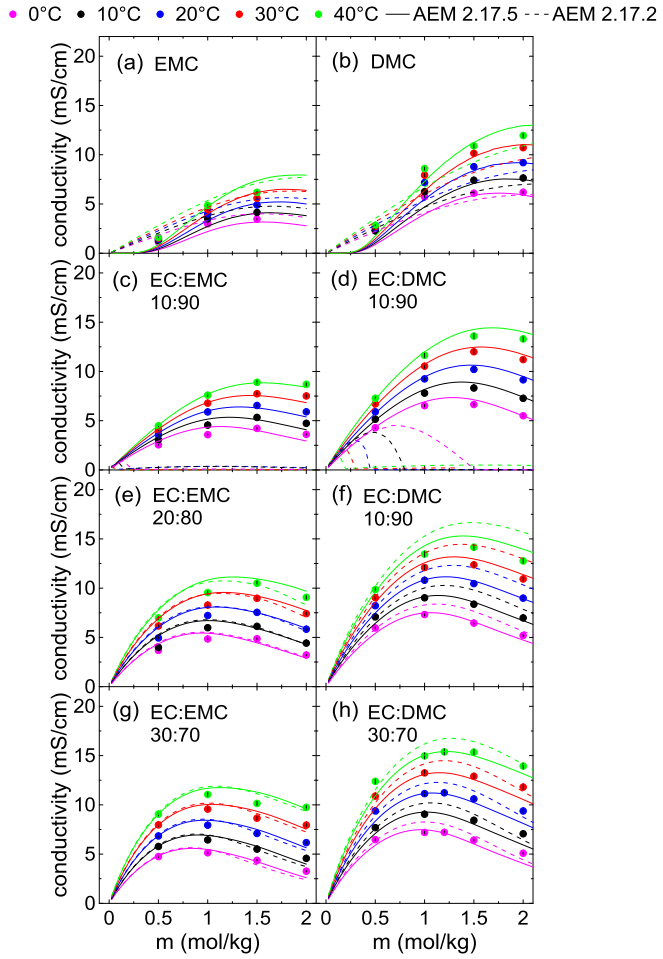

Figure 6. Ionic conductivity as a function of $LiPF_6$ concentration for electrolytes with solvent blends (a) EMC, (b) DMC, (c) EC:EMC 10:90, (d) EC:DMC 10:90, (e) EC:EMC 20:80, (f) EC:DMC 20:80, (g) EC:EMC 30:70, and (h) EC:DMC 30:70, all in weight percent. Temperatures from 0°C to 40°C are shown. Calculations for AEM versions 2.17.2 and 2.17.5 are shown with dashed and solid lines, respectively.

quent rise in the fraction of salt that exists as free ions, thus increasing conductivity.[39,40]

Figures 7 and 8 show (a) the absolute deviation, and (b) the percent deviation of AEM calculations from the experimental viscosity shown in Figures 3 and 5 at 20°C. Figure 7 shows the DMC-containing electrolytes, while Figure 8 shows EMC-containing electrolytes. Different concentrations of $LiPF_6$ are shown as different colors. Different versions of the AEM are specified by different opacities in the bars. The more transparent bars correspond to the older version of AEM, version 2.17.2. This visualization aids in identifying regions in the parameter space where large deviations from experiment may occur. Overall, both the DMC-containing and EMC-containing electrolytes displayed in Figures 7 and 8, respectively, show similar trends with respect to salt concentration and solvent composition. For the electrolyte systems shown in Figure 7, the best agreement with the AEM comes at low salt concentration. Salt-free systems have near perfect agreement with the AEM. This makes sense since the AEM treats the viscosities of mixed solvent systems (no salt added) using a simple mixing rule, while salt-containing systems must consider more complicated ion-ion, solvent-ion, and solvent-solvent interactions.[21]

Previous versions of the AEM had issues calculating the viscosity of low permittivity electrolytes, as can be seen in Figures 7 and 8. Here, the deviation from experiment depends strongly on $LiPF_6$ concentration, and is seen for electrolytes containing 0, 10, or even 20% EC. For example, the calculations for 2.0 m $LiPF_6$ in DMC at

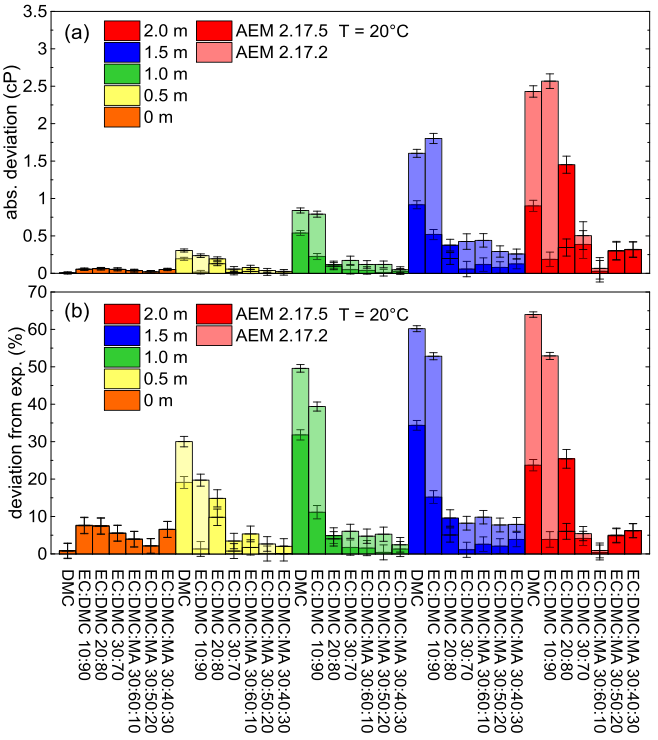

Figure 7. (a) Absolute deviation, and (b) percentage deviation of experimental viscosity values from AEM calculations for electrolytes containing different combinations of EC, DMC, and MA, for different concentrations of $LiPF_6$. Two versions of the AEM are shown, with AEM 2.17.2 as the transparent bars, and AEM 2.17.5 as the solid bars. All results shown are at 20°C.

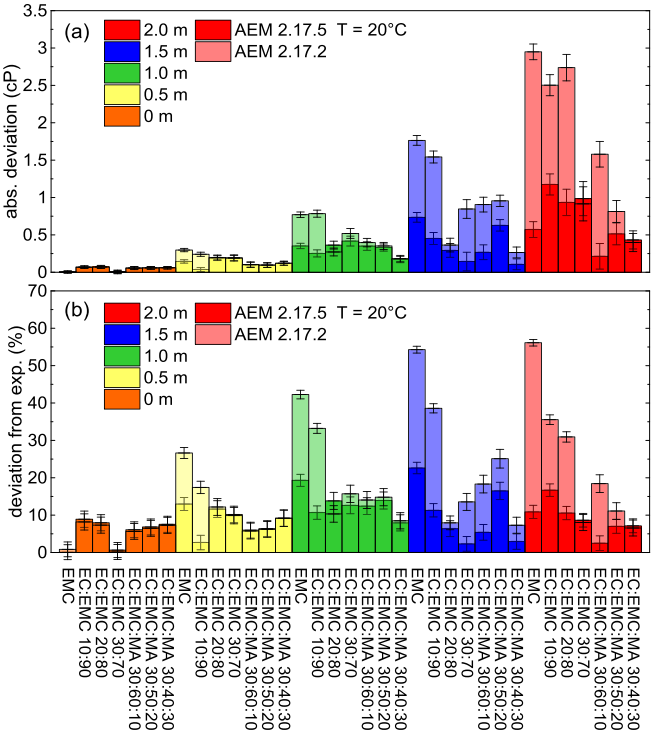

Figure 8. (a) Absolute deviation, and (b) percentage deviation of experimental viscosity values from AEM calculations for electrolytes containing different combinations of EC, EMC, and MA, for different concentrations of $LiPF_6$. Two versions of the AEM are shown, with AEM 2.17.2 as the transparent bars, and AEM 2.17.5 as the solid bars. All results shown are at 20°C.

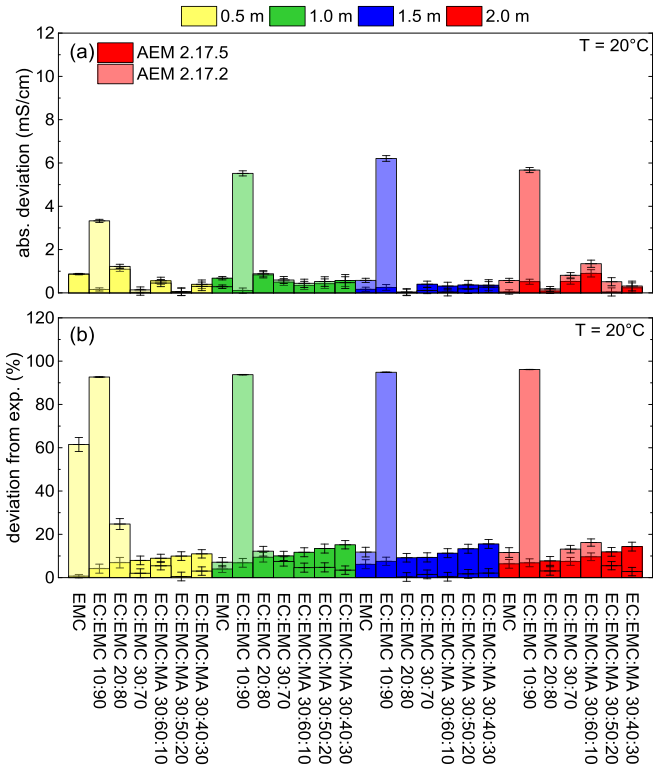

Figure 9. (a) Absolute deviation, and (b) percentage deviation of experimental conductivity values from AEM calculations for electrolytes containing different combinations of EC, EMC, and MA, for different concentrations of $LiPF_6$. Two versions of the AEM are shown, with AEM 2.17.2 as the transparent bars, and AEM 2.17.5 as the solid bars. All results shown are at 20°C.

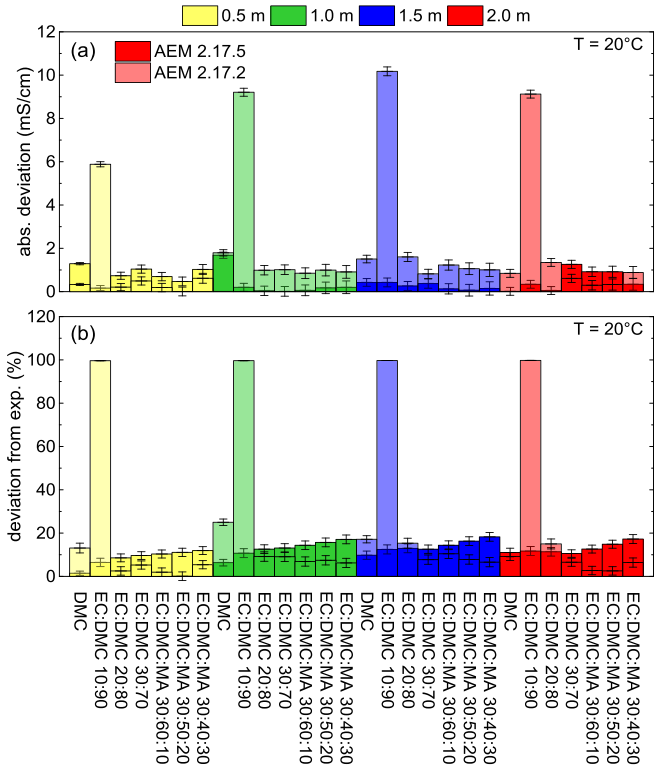

Figure 10. (a) Absolute deviation, and (b) percentage deviation of experimental conductivity values from AEM calculations for electrolytes containing different combinations of EC, DMC, and MA, for different concentrations of $LiPF_6$. Two versions of the AEM are shown, with AEM 2.17.2 as the transparent bars, and AEM 2.17.5 as the solid bars. All results shown are at 20°C.

20°C deviated from experiment by over 60% in AEM version 2.17.2. The agreement has been improved between versions 2.17.2 and 2.17.5, however some large disagreements remain for the viscosity of low-EC electrolytes containing high concentrations of $LiPF_6$. Improvements in agreement between these versions relate back to more accurate interpretations of solution permittivity for low-to-no-EC systems. As the model more correctly predicts an increase of free ions that emerge due to the presence of ion pair dipoles, these free ions will be fully solvated and hence increase viscosity more so than charge-neutral ion pairs. During the writing of this manuscript a theoretical term covering the near-neighbor probabilities was added to AEM solution permittivity calculations and was seen to produce much greater accuracy of viscosity and conductivity of low-permittivity electrolytes, especially at low salt concentrations.

Figures 9 and 10 show deviation of AEM calculations from measured conductivity values shown in Figures 4 and 6. Figure 9 shows (a) absolute deviation, and (b) percent deviation from experimental conductivity for EMC-containing electrolytes, and Figure 10 shows the same information for DMC-containing electrolytes. Like in the viscosity results shown in Figures 7 and 8, the trends seen for EMC and DMC-containing electrolytes are very similar in Figures 9 and 10. In AEM version 2.17.2, there was a very large deviation from experiment for electrolytes containing 10% EC. This large deviation was seen over the whole concentration range studied. Perhaps surprisingly, this deviation was not seen in any electrolytes with 0% EC, with the exception of 0.5 m $LiPF_6$ in EMC. Much of these deviations have been addressed in subsequent versions of the AEM. It should be noted that although the very large deviations at 10% EC have been addressed, between AEM versions 2.17.2 and 2.17.5, deviations from experiment increased slightly for solvent compositions containing 30% EC and different proportions of MA. This is seen across EMC and DMC-containing electrolytes as well as the full range of $LiPF_6$ concentrations examined. For those compositions where agreement to experiment became slightly worse between AEM versions, the percentage deviation is still less than 20% for all compositions. Overall, the AEM's agreement with experiment in its current version is very good for electrolytes with varying permittivity (EC content) and $LiPF_6$ concentrations.

AEM version 2.17.5 is able to predict the conductivity and viscosity of the above mentioned electrolyte systems with good accuracy. This version of the AEM is now compared with the large catalog of data found in Dudley et al.[5] Figure 11 shows ionic conductivity as a function of temperature for electrolytes of various solvent combinations containing LiTf as the conducting salt. Figure 12 shows ionic conductivity as a function of temperature for electrolyte mixtures with sulfolane as the sole solvent, and different concentrations of $LiAsF_6$, again measured by Dudley et al. In both Figures 11 and 12, calculations from AEM version 2.17.5 are shown as dashed lines, and calculations from a newer version of the program, version 2.18.1, are shown as solid lines. These two sets of electrolytes were chosen to display the full conductivity-temperature data first to give an appropriate sample of the different systems considered in Dudley et al., and second to show the improvements in AEM agreement for these systems. It can be seen from these two Figures that the initial agreement of AEM version 2.17.5 with these systems was quite poor especially for the systems containing LiTf (Figure 11). This large discrepancy has been addressed in the subsequent version of the AEM, as seen from the solid lines in Figures 11 and 12. These improvements were accomplished by assigning more accurate molecular interaction parameters to each of the solvent-ion combinations through standard reference ligand lengths and solvent residence times around ions.

Figures 13 and 14 show (a) the absolute deviation, and (b) the percent deviation of the AEM from the experimental conductivity values found in Dudley et al. Calculations from AEM 2.17.5 are given as transparent bars, while calculations from AEM version 2.18.1 are shown as solid bars. Figure 13 shows electrolyte solutions with salt

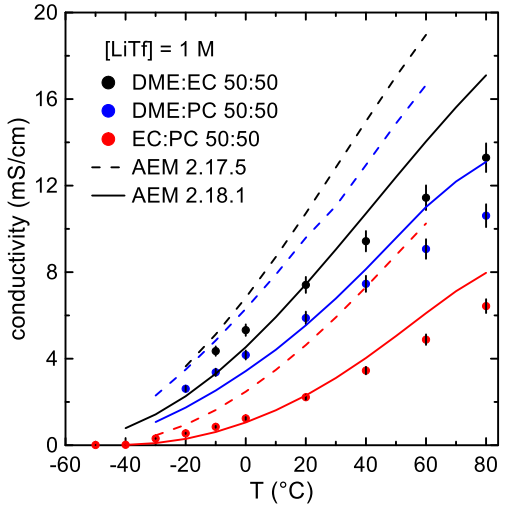

Figure 11. Conductivity as a function of temperature for electrolytes containing the Li triflate salt from Dudley et al.[5] Solvent compositions are given as volume fractions. Calculations from AEM version 2.17.5 are shown as dashed lines, and calculations from AEM version 2.18.1 are shown as solid lines.

concentrations of 1.0 M, while Figure 14 shows solutions with [LiX] $\neq$ 1.0 M, with X representing the various anions in the salts used in Dudley et al.[5] As was seen before in Figures 7–10, there is little discrepancy between the absolute and percent deviations given in panels (a) and (b), respectively. Large deviations that appear in the percent deviation plot also show up in the absolute deviation plot. First looking at salt concentrations of 1 M only (Figure 13), in AEM version 2.17.5, some of the biggest deviations from experimental conductivity values were for electrolytes containing the solvent sulfolane (tetramethylene sulfone, TMS), and electrolytes with the salt LiTf. Most of these notably large deviations have been improved in AEM version 2.18.1. However, while the especially large deviations have been eliminated, there are some systems where the deviation from experiment became larger in AEM version 2.18.1. Most of the electrolyte systems that saw an increased deviation between versions contained sulfolane as a solvent, along with either diglyme or DME. These trends in the deviations suggest that further optimization is needed for the molecular interaction parameters (solvent-ion reference ligand lengths and solvent residence times) of these electrolyte components.

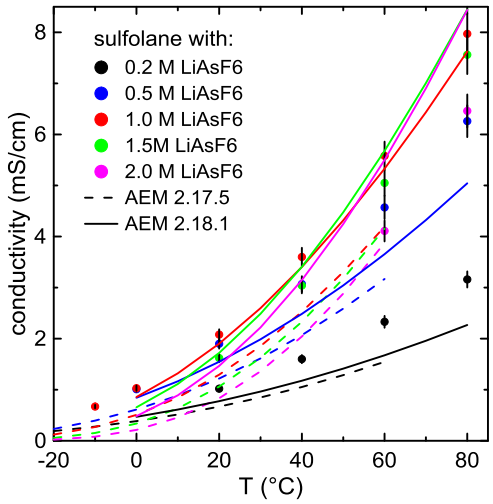

Figure 12. Ionic conductivity as a function of temperature for electrolytes containing sulfolane as the sole solvent for different concentrations of $LiAsF_6$. Calculations from AEM version 2.17.5 are shown as dashed lines, and calculations from AEM version 2.18.1 are shown as solid lines.

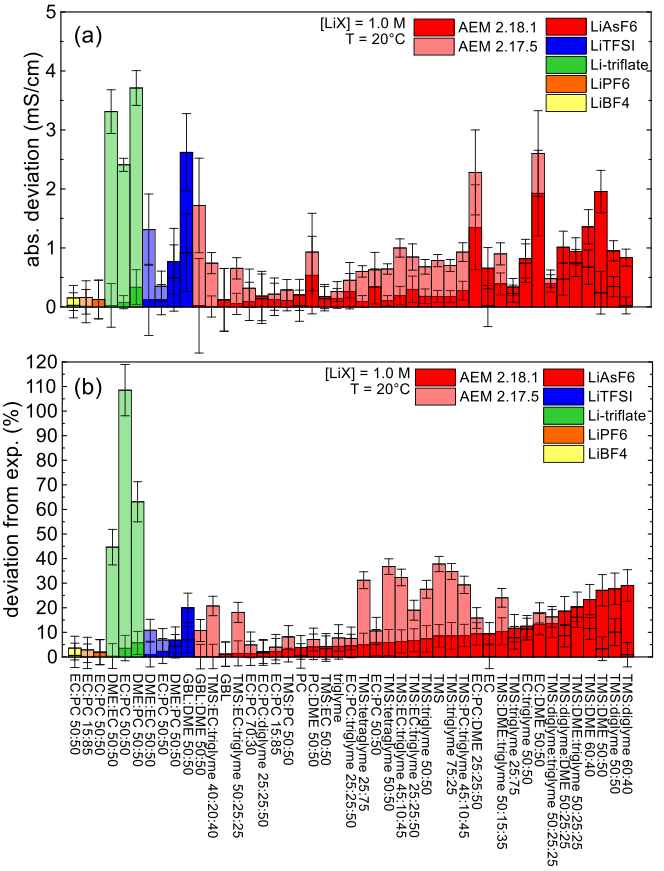

Figure 13. A summary of (a) absolute deviation, and (b) percentage deviation of AEM calculations from experimental conductivity values for the various electrolytes studied in Dudley et al.[5] Calculations from AEM version 2.17.5 are shown as transparent bars, and calculations from AEM version 2.18.1 are displayed as solid bars. Different Li salts are shown, specified by the color of the bar. The concentration of Li salt for all electrolytes in this Figure is 1.0 M. All results are shown at 20°C.

There were far fewer electrolyte systems tested with salt concentrations other than 1 M in Dudley et al (Figure 14). There does appear to be a dependence of salt concentration on deviation from the model, with many of the systems with the highest deviations have Li salt concentrations $>$ 1 M. However, this should not be taken as a general rule, since the systems with 4 M $LiAsF_6$ have relatively low deviations from experiment. For these non-unity salt concentration systems, it appears that AEM 2.18.1 either keeps constant or improves the agreement with experiment compared to the previous version. While some systems do still have large deviations, the updated version of the AEM shows a marked improvement in general.

Improvements in AEM accuracy.—The AEM has been shown to achieve accuracy over a wide assortment of electrolyte compositions and conditions. There are two fundamental routes to further improve accuracy. First, theory can be improved that covers a particular property set. This was seen quite dramatically for EC-free electrolytes when the AEM solution permittivity calculations were revised to include the impact from ion pair dipoles. Other recent improvements to AEM theory (not demonstrated here) capture the effects of very high salt concentrations (above 4M) and colligative solvation of ion associated members. The second route to improved AEM performance is through more accurate molecular interaction parameters. As mentioned above, AEM utilizes, as a reference state, solvent-ion ligand lengths and solvent residence times (defined at infinite dilution

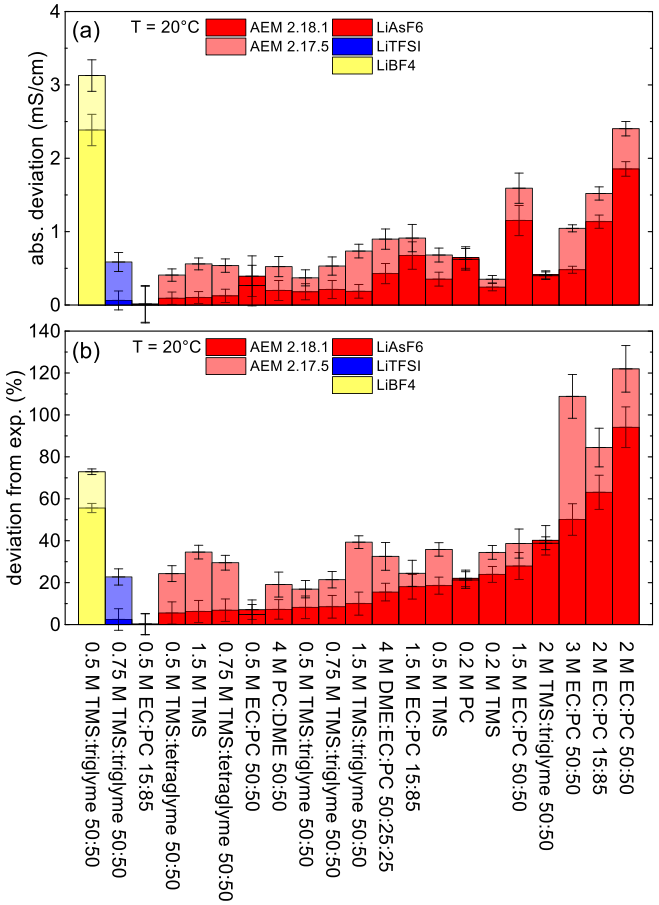

Figure 14. A summary of (a) absolute deviation, and (b) percentage deviation of AEM calculations from experimental conductivity values for the various electrolytes studied in Dudley et al.[5] Calculations from AEM version 2.17.5 are shown as transparent bars, and calculations from AEM version 2.18.1 are displayed as solid bars. Different Li salts are shown, specified by the color of the bar. Salt concentrations other than 1.0 M are shown. All results are shown at 20°C.

salt and 298.15 K) as a means to quantify solvent-ion interactions. Solvent shape, size and orientation to a given ion factors into these terms. When these molecular parameters are optimized, the AEM can predict electrolyte properties to very good accuracy. Most of the cases where successive versions of AEM were used in comparison to Dudley et al.[5] show the benefit of better optimized molecular parameters. This optimization is made possible by high-quality data obtained at precisely known conditions. In most instances, only a few data points are needed to obtain satisfactory values of AEM parameters, while for other systems, pre-validation estimates for these parameters have produced initial property predictions very close to measured values.

Conclusions

The purpose of this paper was to highlight the strengths and weaknesses of the Advanced Electrolyte Model (AEM) over a wide range of electrolyte systems. Care was taken not to purposefully pick exemplary electrolyte systems that showed either good or bad agreement, thus the reason for investigating both novel and obsolete systems. The authors believe that this set of comparator data provides an honest evaluation of the AEM as of summer 2018, and also highlights the contributions made by experimental validation of the model to further improve the program. The AEM now provides good predictions of the basic transport properties (conductivity and viscosity) of the various electrolyte systems studied. Significant improvements to AEM were most notably in the region of low-permittivity electrolytes.

Ionic conductivity and electrolyte viscosity are only two of the many quantities that the AEM computes for a given electrolyte system. Other electrolyte properties such as diffusivity (all species), transference number, activity coefficients, solvent and solution permittivities, solvent-ion binding energies, etc. speak to additional valuable attributes of electrolytes and can be selection criteria as well. Since the same chemical physics platform is used for these other properties as is used for viscosity and conductivity, commensurate accuracy of the other properties is anticipated. However, model validation is required with each new property or electrolyte system to test the robustness of the AEM. In order to validate the entirety of the model, these quantities must also be compared to experiment, provided there is a clear basis for comparison between lab and model results, as is being done at Dalhousie University and elsewhere. Validation of other transport parameters provided by the AEM will be the subject of a forthcoming publication.

Acknowledgments

The authors thank NSERC and Tesla Canada for funding under the auspices of the Industrial Chairs program. E.R.L. thanks the Nova Scotia graduate scholarship program for support and E.M.T. thanks NSERC for support under the USRA program. K.L.G acknowledges support from INL Technology Deployment to further his collaboration with Dalhousie University.

ORCID

J. R. Dahn https://orcid.org/0000-0002-6997-2436

References

1. S. Stewart and J. Newman, *J. Electrochem. Soc.*, **155**, A458 (2008).
2. A. Ehrl, J. Landesfeind, W. A. Wall, and H. A. Gasteiger, *J. Electrochem. Soc.*, **164**, A826 (2017).
3. A. Ehrl, J. Landesfeind, W. A. Wall, and H. A. Gasteiger, *J. Electrochem. Soc.*, **164**, A2716 (2017).
4. L. O. Valøen and J. N. Reimers, *J. Electrochem. Soc.*, **152**, A882 (2005).
5. J. T. Dudley, D. P. Wilkinson, G. Thomas, R. LeVae, S. Woo, H. Blom, C. Horvath, M. W. Juzkow, B. Denis, P. Juric, P. Aghakian, and J. R. Dahn, *J. Power Sources*, **35**, 59 (1991).
6. E. R. Logan, E. M. Tonita, K. L. Gering, J. Li, X. Ma, L. Y. Beaulieu, and J. R. Dahn, *J. Electrochem. Soc.*, **165**(2), A21 (2018).
7. E. R. Logan, E. M. Tonita, K. L. Gering, L. Ma, M. K. G. Bauer, J. Li, L. Y. Beaulieu, and J. R. Dahn, *J. Electrochem. Soc.*, **165** (3), A705 (2018).
8. A. Nyman, M. Behm, and G. Lindbergh, *Electrochim. Acta*, **53**, 6356 (2008).
9. M. S. Ding, *J. Chem. Eng. Data.*, **48**, 519 (2003).
10. M. S. Ding and T. R. Jow, *J. Electrochem. Soc.*, **150**, A620 (2003).
11. M. S. Ding and T. R. Jow, *J. Electrochem. Soc.*, **151**, A2007 (2004).
12. M. S. Ding, *J. Chem. Eng. Data.*, **49**, 1102 (2004).
13. M. Dahbi, F. Ghamouss, F. Tran-Van, D. Lemordant, and M. Anouti, *J. Power Sources*, **196**, 9743 (2011).
14. H. G. Schweiger, M. Multerer, M. Schweizer-Berberich, and H. J. Gores, *J. Electrochem. Soc.*, **152**, A577 (2005).
15. M. S. Ding, K. Xu, S. S. Zhang, K. Amine, G. L. Henriksen, and T. R. Jow, *J. Electrochem. Soc.*, **148**, A1196 (2001).
16. T. R. Jow, M. S. Ding, K. Xu, S. S. Zhang, J. L. Allen, K. Amine, and G. L. Henriksen, *J. Power Sources*, **119–121**, 343 (2003).
17. C. H. Yim, J. Tam, H. Soboleski, and Y. Abu-Lebdeh, *J. Electrochem. Soc.*, **164**, A1002 (2017).
18. L. F. Xiao, Y. L. Cao, X. P. Ai, and H. X. Yang, *Electrochim. Acta*, **49**, 4857 (2004).
19. K. Xu, *Chem. Rev.*, **104**, 4303 (2004).
20. L. Y. Beaulieu, E. R. Logan, K. L. Gering, and J. R. Dahn, *Rev. Sci. Instrum.*, **88**, 095101 (2017).
21. K. L. Gering, *Electrochim. Acta*, **51**, 3125 (2006).
22. K. L. Gering, *Electrochim. Acta*, **225**, 175 (2017).
23. R. Petibon, C. P. Aiken, L. Ma, D. Xiong, and J. R. Dahn, *Electrochim. Acta.*, **154**, 287 (2015).
24. R. Petibon, J. Harlow, D. B. Le, and J. R. Dahn, *Electrochim. Acta.*, **154**, 227 (2015).
25. R. Petibon, J. Xia, L. Ma, M. K. G. Bauer, K. J. Nelson, and J. R. Dahn, *J. Electrochem. Soc.*, **163**(13), A2571 (2016).
26. X. Ma, J. Li, S. L. Glazier, L. Ma, K. L. Gering, and J. R. Dahn, *Electrochim. Acta*, **270**, 215 (2018).
27. X. Ma, R. S. Arumugam, L. Ma, E. Logan, E. Tonita, J. Xia, R. Petibon, S. Kohn, and J. R. Dahn, *J. Electrochem. Soc.*, **164**, A3556 (2017).

28. M. C. Smart, B. V. Ratnakumar, K. B. Chin, and L. D. Whitcanack, *J. Electrochem. Soc.*, **157**, A1361 (2010).
29. M. C. Smart, B. V. Ratnakumar, and S. Surampudi, *J. Electrochem. Soc.*, **149**, A361 (2002).
30. M. C. Smart, B. V. Ratnakumar, S. Surampudi, Y. Wang, X. Zhang, S. G. Greenbaum, A. Hightower, C. C. Ahn, and B. Fultz, *J. Electrochem. Soc.*, **146**, 3963 (1999).
31. J. Xia, R. Petibon, D. Xiong, L. Ma, and J. R. Dahn, *J. Power Sources*, **328**, 124 (2016).
32. L. Ma, S. L. Glazier, R. Petibon, J. Xia, J. M. Peters, Q. Liu, J. Allen, R. N. C. Doig, and J. R. Dahn, *J. Electrochem. Soc.*, **164**, A5008 (2017).
33. J. Li, H. Li, X. Ma, W. Stone, S. Glazier, E. Logan, E. M. Tonita, K. L. Gering, and J. R. Dahn, *J. Electrochem. Soc.*, **165** (5), A1027 (2018).
34. Y.-G. Cho, Y.-S. Kim, D.-G. Sung, M.-S. Seo, and H. K. Song, *Energy Environ. Sci.*, **7**, 1737 (2014).
35. L. Zhou, M. Xu, and B. L. Lucht, *J. Appl. Electrochem.*, **43**, 497 (2013).
36. D. S. Hall, A. Eldesoky, E. R. Logan, E. M. Tonita, X. Ma, and J. R. Dahn, *J. Electrochem. Soc.*, **165**(10) A2365 (2018).
37. J. Self, B. M. Wood, N. N. Rajput, and K. A. Persson, *J. Phys. Chem. C*, **122**, 1990 (2018).
38. D. J. Xiong, T. Hynes, and J. R. Dahn, *J. Electrochem. Soc.*, **164**, A2089 (2017).
39. M. Delsignore, H. Farber, and S. Petrucci, *J. Phys. Chem.*, **89**, 4968 (1985).
40. L. Doucey, M. Revault, A. Lautié, A. Chaussé, and R. Messina, *Electrochim. Acta*, **44**, 2371 (1999).